Journal of Experimental Marine Biology and Ecology 390 (2010) 84–98

Contents lists available at ScienceDirect

Journal of Experimental Marine Biology and Ecology

journal homepage: www.elsevier.com/locate/jembe

To go or not to go with the flow: Environmental influences on whale shark movement patterns

Jai C. Sleeman [a,*], Mark G. Meekan [b], Steven G. Wilson [c], Jeffrey J. Polovina [d], John D. Stevens [e], Guy S. Boggs [a], Corey J.A. Bradshaw [f,g]

[a] GIS and Remote Sensing Group, Charles Darwin University, Darwin, Northern Territory 0909, Australia
[b] Australian Institute of Marine Science, P.O. Box 40197, Casuarina MC, Northern Territory 0811, Australia
[c] Hopkins Marine Laboratory, Stanford University, 120 Oceanview Blvd., Pacific Grove, CA 93950, USA
[d] National Marine Fisheries Service, Pacific Islands Fisheries Science Center, Honolulu, HI, USA
[e] CSIRO Marine and Atmospheric Research, G.P.O. Box 1538, Hobart, Tasmania 7001, Australia
[f] The Environment Institute and School of Earth and Environmental Sciences, University of Adelaide, Adelaide, South Australia 5005, Australia
[g] South Australian Research and Development Institute, P.O. Box 120, Henley Beach, South Australia 5022, Australia

ARTICLE INFO

Article history:
Received 13 November 2009
Accepted 18 May 2010

Keywords:
Geostrophic currents
Migration
Oceanography
Passive diffusion model
Rhincodon typus
Satellite tracking

ABSTRACT

Seven whale sharks were tracked using satellite-linked tags from Ningaloo Reef, off northern Western Australia, following tagging in April and June 2002 and April–May 2005. We investigated how the movements of those whale shark tracks were influenced by geostrophic surface currents during sequential one-week periods by using a passive diffusion model parameterised with observed starting locations of the sharks and weekly maps of surface current velocity and direction (derived from altimetry). We compared the outputs from the passive diffusion model and maps of chlorophyll-*a* concentration (SeaWiFs/MODIS) and with the actual tracks of the sharks using GIS and generalized linear mixed-effects models (GLMM). The GLMM indicated very little support for passive diffusion with sea-surface ocean currents influencing whale shark distributions in the north eastern Indian Ocean. Moreover, the sharks' movements correlated only weakly with the spatial distribution of sea-surface chlorophyll-*a* concentrations. The seven whale sharks had average swimming speeds comparable with those recorded in other satellite tracking studies of this species. Swimming speeds of the seven sharks were similar to those reported in previous studies and up to three times greater than the maximum sea-surface current velocities that the sharks encountered while traversing into lower southerly latitudes (moving northward towards the equator). Our results indicate that whale sharks departing from Ningaloo travel actively and independently of near-surface currents where they spend most of their time despite additional metabolic costs of this behaviour.

1. Introduction

It has been hypothesized that many migratory marine animals including birds, cetaceans (Ballance et al., 2006), turtles (Polovina et al., 2000, 2004; Luschi et al., 2003; Gaspar et al., 2006; Lambardi et al., 2008; Shillinger et al., 2008) and sharks (Montgomery and Walker, 2001; Sims et al., 2003) use geophysical directional clues such as the Earth's magnetic field and thermoreception of large water temperature gradients associated with fronts and eddies for navigation. For example, the basking shark (*Cetorhinus maximus* Gunnerus) is a large filter-feeding migratory shark that actively seeks out productive biological habitats along the continental shelf over areas of several hundred to thousand kilometres to forage in temporally discrete, high productivity areas associated with ocean fronts (Sims, 2003). Similarly, the broad-scale migrations of several species of marine turtles are influenced by oceanographic processes. Olive ridley (*Lepidochelys olivacea*) and leatherback (*Dermochelys coriacea*) turtles have been shown to use major surface currents and eddies to assist migration to feeding areas (Polovina et al., 2000, 2004; Luschi et al., 2003).

Whale sharks (*Rhincodon typus* Smith) are the world's largest fishes and are broadly distributed throughout tropical and subtropical oceans. These animals are highly migratory, travelling large distances (thousands of km, Rowat and Gore, 2007; Eckert and Stewart, 2001) and appear predictably at some coastal localities in the tropics to take advantage of ephemeral increases in the abundance of their zooplankton prey (Heyman et al., 2001; Wilson et al., 2001; Meekan et al., 2006).

* Corresponding author.
E-mail address: jai.sleeman@cdu.edu.au (J.C. Sleeman).

0022-0981/$ – see front matter © 2010 Elsevier B.V. All rights reserved.
doi:10.1016/j.jembe.2010.05.009

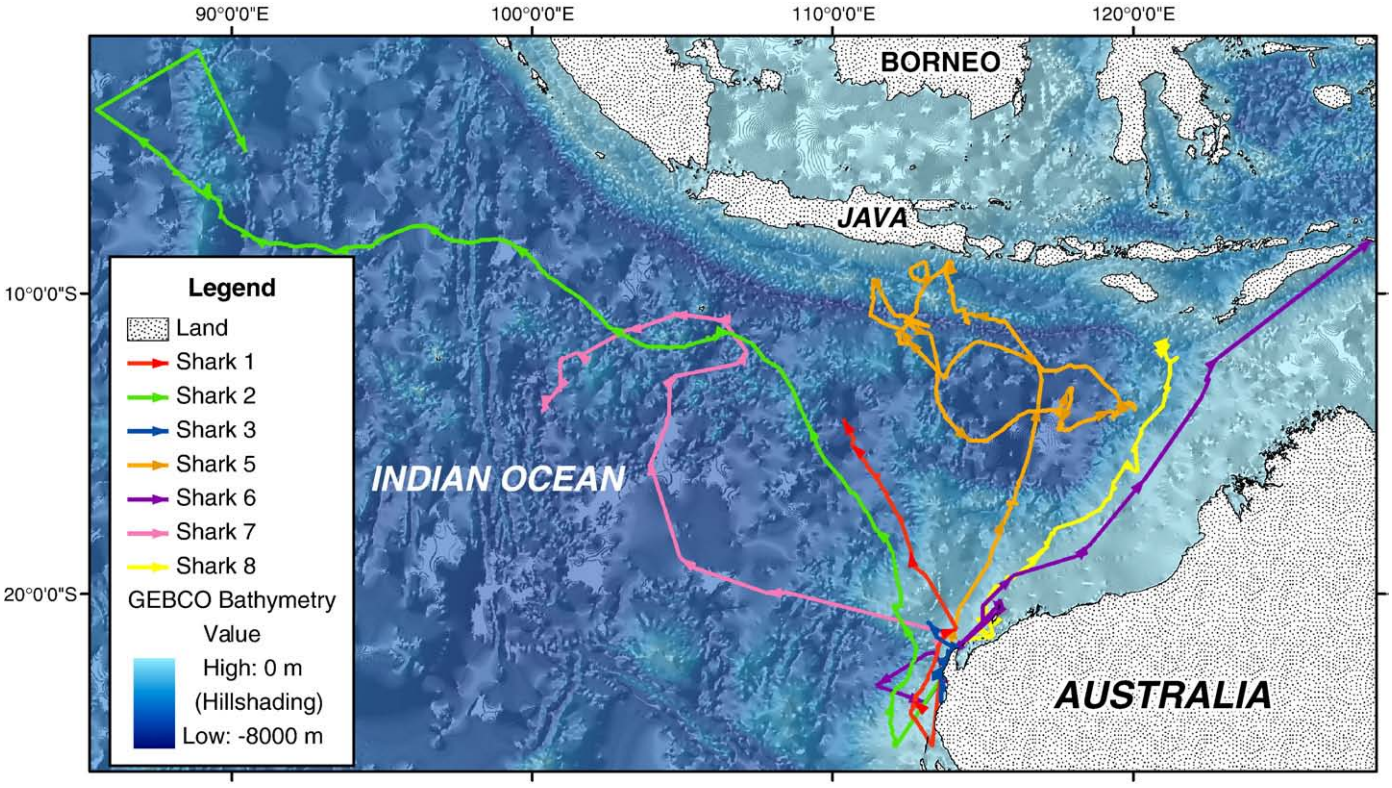

Fig. 1. Distribution of whale shark tracks in the Indian Ocean and associated bathymetry.

It remains a mystery how whale sharks navigate to and from these aggregation sites and whether they use active locomotion or they are assisted via passive drifting in currents. We examined this issue by comparing the movements of whale sharks monitored with satellite-linked transmitter tags and sea-surface geostrophic currents and chlorophyll-*a* concentration gradients during weekly intervals to test

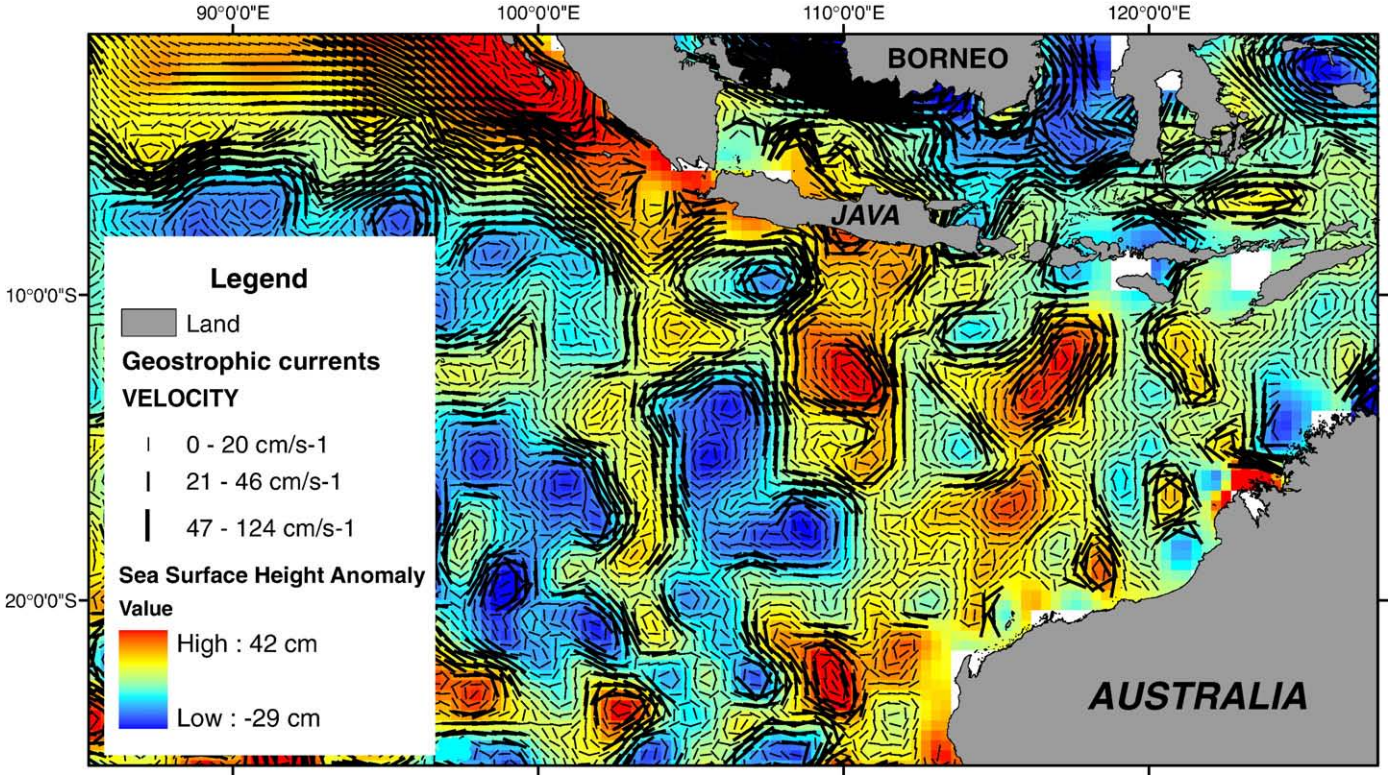

Fig. 2. Example of geostrophic current map (velocity cm/s^{-1}) for the mid Austral winter period (June 2005).

Table 1
Model comparison using Akaike's Information Criterion corrected for small sample size (AIC_c) and Bayesian Information Criterion (BIC). Shown are the model terms (PMP = passive-movement cell occupancy probability; CHL = chlorophyll-*a* concentration), number of parameters (*k*), maximum log-likelihood, deviance in criterion scores from top-ranked models (ΔAIC_c and ΔBIC), information criteria weights ($wAIC_c$ and *w*BIC) and the per cent deviance explained (%DE) by each model.

No.	Model	*k*	*LL*	ΔAIC_c	$wAIC_c$	ΔBIC	*w*BIC	%DE
1	~PMP + CHL	5	−581.557	0.000	0.432	4.146	0.086	0.99
2	~CHL	4	−582.726	0.306	0.371	0.000	0.686	0.79
3	~PMP + CHL + PMP*CHL	6	−581.552	2.026	0.159	10.618	0.003	0.99
4	~PMP	4	−585.219	5.292	0.031	4.986	0.057	0.37
5	~1 (null)	3	−587.380	7.589	0.010	2.824	0.167	0.0

the null hypotheses: (i) that whale shark movements from Ningaloo Reef north Western Australia are independent of sea-surface ocean currents and; (ii) that whale shark residency patterns are independent of near-surface local productivity measures (i.e., remotely assessed chlorophyll-*a* concentrations).

2. Materials and methods

2.1. Tagging

Observers in single engine, high wing aircraft were used to locate whale sharks and direct a boat with snorkelers to them in 2002 and 2005 (see Wilson et al., 2006). Once the sharks were located, satellite-linked radio transmitter SPLASH Tags (Wildlife Computers, Redmond, USA) were attached to the leading dorsal fins of seven whale sharks (a 7-m female whale shark on 22 April 2002, a 7-m male on 28 June 2002, and five individuals — 2 female, 1 male, and 2 of undetermined sex ranging in total length from 4.2 to 7.5 m from 1–6 May 2005) near Point Cloates, Ningaloo Reef (113° 36′ E, 22° 42′ S) in Western Australia (Fig. 1). The SPLASH tags were embedded in a 33 cm long buoyant torpedo-shaped housing manufactured from syntactic foam that was attached to a delron collar via a 1-metre stainless steel tether. A snorkeler attached the delron collar to the whale shark a handheld, pressure-driven applicator (RAMSET) that secured the collar to the shark's dorsal fin by a stainless steel pin and plastic saddle (Wilson et al., 2006). Tag application techniques were developed at CSIRO Marine and Atmospheric Research in accordance with methods to minimize tag loss and with adherence to animal ethics guidelines.

The transmitters were radio-silent when submerged owing to a sea-water conductivity circuit but transmitted spontaneously once the tag breached the sea-surface and continued to transmit at 45 s intervals as long as at least one of the circuit electrodes was dry. The tag's locations were determined by the ARGOS Data Collection and Location Service (DCLS) by Doppler shift in transmissions received by the orbiting ARGOS DCLS satellites (Stewart et al., 1989; Eckert and Stewart, 2001). Summary histogram on diving depth and water temperature covering 6-hour periods were also transmitted through the ARGOS DCLS.

Whale shark location data were filtered to eliminate poor quality locations where predicted accuracy (based on satellite triangulation) was >1 km. This level of filtering (sub-kilometer) was deemed appropriate for including locations that were well within spatial guidelines of minimum resolution (i.e. at least 5 times smaller than the minimum resolution of other environmental data sets used for spatial comparison/modeling, O'Neill et al., 1996). Point location data and diving data were evaluated to determine when the tags separated from whale sharks and began drifting at the sea-surface. Locations were divided into weekly intervals that corresponded with environmental data of similar periods and time-frames. Point data were imported into ArcGIS v9.1 (ESRI, Redlands, USA) and interpolated (assuming linear movement between points) into track lines where points were used as vertices. The average precision of interpolated locations from marine animals with ARGOS-linked tags have been found to be unaffected by various interpolation methods and were always within the precision of the tracking technique (Tremblay et al., 2006). For each shark we calculated the distance that it traveled over a week (km), the time interval between location reports (hours) and the travel speed (km hr). These data were joined to a vector grid (with cell sizes of 0.1° latitude/longitude or ~36 km, equal to geostrophic current data) using the Hawths Tools ArcGIS extension. By summing the time spent within each vector grid cell we created an observed probability density time series grid for each whale shark. We also calculated average heading direction (relative to True North) for all weekly tracks of individual whale sharks.

2.2. Environmental data

Geostrophic surface currents are generated by differences in horizontal pressure gradients associated with sea-surface topography and the Coriolis force. To estimate weekly surface geostrophic currents for locations corresponding to the whale shark tracks, we obtained altimetry data (www.aviso.oceanobs.com) with a spatial resolution of 0.1° (latitude/longitude). Coastal processes operating within the coastal strip, an approximately 36 km-wide band of ocean adjacent to the coast, produce noise in altimetry data making it difficult to resolve sea-surface height in this region. The derivation of geostrophic current maps from altimetry adds to the problem of missing data by utilizing a neighbourhood function that relies on adjacent grid cells that further degrades the outer edge of the map extent. As a consequence of this, geostrophic current maps can only be created for offshore waters at least 0.1° (longitude/latitude) or ~36 km beyond the coastline.

We used geoprocessing tools in ArcGIS to spatially intersect (join) whale shark tracks with underlying geostrophic current grid cell

Table 2
Comparison of tagged whale sharks, sex (F = female, M = male, ? = unknown), total track length (km) and the average movement speeds of whale sharks (km h^{-1}) with average, mode, minimum and maximum of geostrophic current velocities (km h^{-1}) within their observed migration routes.

Shark ID	Sex	Total track length (km)	Average speed of sharks (km h^{-1})	Average velocity of geostrophic currents (km h^{-1})	Mode of geostrophic current velocity (km h^{-1})	Minimum geostrophic current velocity (km h^{-1})	Maximum geostrophic current velocity (km h^{-1})
1	F	2003.84	2.41	0.22	0.41	0.05	0.82
2	M	6384.76	1.74	0.47	0.58	0.04	1.51
3	?	1209.02	1.17	0.35	0.32	0.32	0.81
5	F	6595.08	1.89	0.51	0.38	0.03	1.81
6	?	3944.63	1.36	0.47	0.74	0.19	1.34
7	F	3441.76	1.63	0.44	0.52	0.02	1.60
8	M	2681.19	3.19	0.31	0.27	0.03	1.60

values (velocity and direction). Histograms were created from these intersected data to get an indication of the range of oceanographic variables surrounding weekly tracks. Using a raster calculator in ArcGIS, we multiplied mean sea level anomalies by their formal mapping errors (variance in sensor signal) to estimate minimum and maximum mean sea level height per grid cell. These limits were added to a mean dynamic topography grid based on a geoid model (Rio and Hernandez, 2004) and the resulting absolute dynamic topography maps were reprojected into a Mercator equal-area projection and east–west (dz/dx) and north–south (dz/dy) gradients calculated using a filter in ArcView 3.2 (ESRI, Redlands, California, USA). Gradient maps were exported in geographic coordinates to calculate the geostrophic current components of the north–south (U) and east–west (V) (Polovina et al., 1999) and these were decomposed into compass direction (degrees True North) and velocity ($cm\ s^{-1}$) (Fig. 2).

Maps of chlorophyll-*a* concentration were used as an index of biological surface water productivity along whale shark movement trajectories. Weekly chlorophyll-*a* maps with 9-km spatial resolution were derived from Sea-viewing Wide Field-of-view Sensor (SeaWiFS) level 3 (version 5.1) Global Area Coverages (GAC). SeaDAS 4.8 ocean color software (developed by the US National Aeronautics and Space Administration), was used to georeference and subset chlorophyll-*a* imagery for the entire region within which whale sharks tracks occurred.

2.3. Passive diffusion model

We developed an agent-based, passive current diffusion model using the *R* Package (R Development Core Team, 2004). The model was based on weekly minimum and maximum geostrophic current velocity and direction maps and a land-mask map as inputs. Inputs for each weekly model scenario were based on the *x* and *y* coordinates or actual surface locations of whale sharks when first recorded outside the coastal strip (the available geographic coverage of altimetry/geostrophic current data).

The model simulated movement of an agent (whale shark) through a grid-based environment where each daily time step (within a weekly interval) was evaluated on the basis of the grid cell length (distance) according to the velocity and direction values of geostrophic currents in neighbouring cells and whether the cells could be occupied or not (based on the land-mask). *R*-code for this procedure is available from the authors upon request. The model assumed that the whale sharks had no resistance associated with their shape or surface area/volume ratio to being propelled at the same speed and in the same flow direction as the geostrophic currents.

Geostrophic map data were reprojected into an Albers equidistant conic projection prior to input to ensure that simulated whale shark movements into adjacent cells were standardised in both the east–west and north–south directions. The model was coded as a stochastic process where variation of geostrophic current estimates (associated with formal mapping errors) were incorporated as 100 iterations of daily steps for each weekly interval and randomly sampling velocity and direction values within their error ranges (coefficient of variation for velocity and direction set at 0.25). A cumulative cell occupancy output map was generated following 100 iterations to generate a passive agent surface occupancy probability density. We produced one cumulative cell occupancy output map for each week where the model was initiated from the actual shark starting location for that week.

All weekly cumulative cell occupancy output maps that were predicted for individual sharks were added together to produce a final cumulative cell occupancy map.

We then extracted surface current probability values and average chlorophyll-*a* concentrations at cell locations that corresponded to

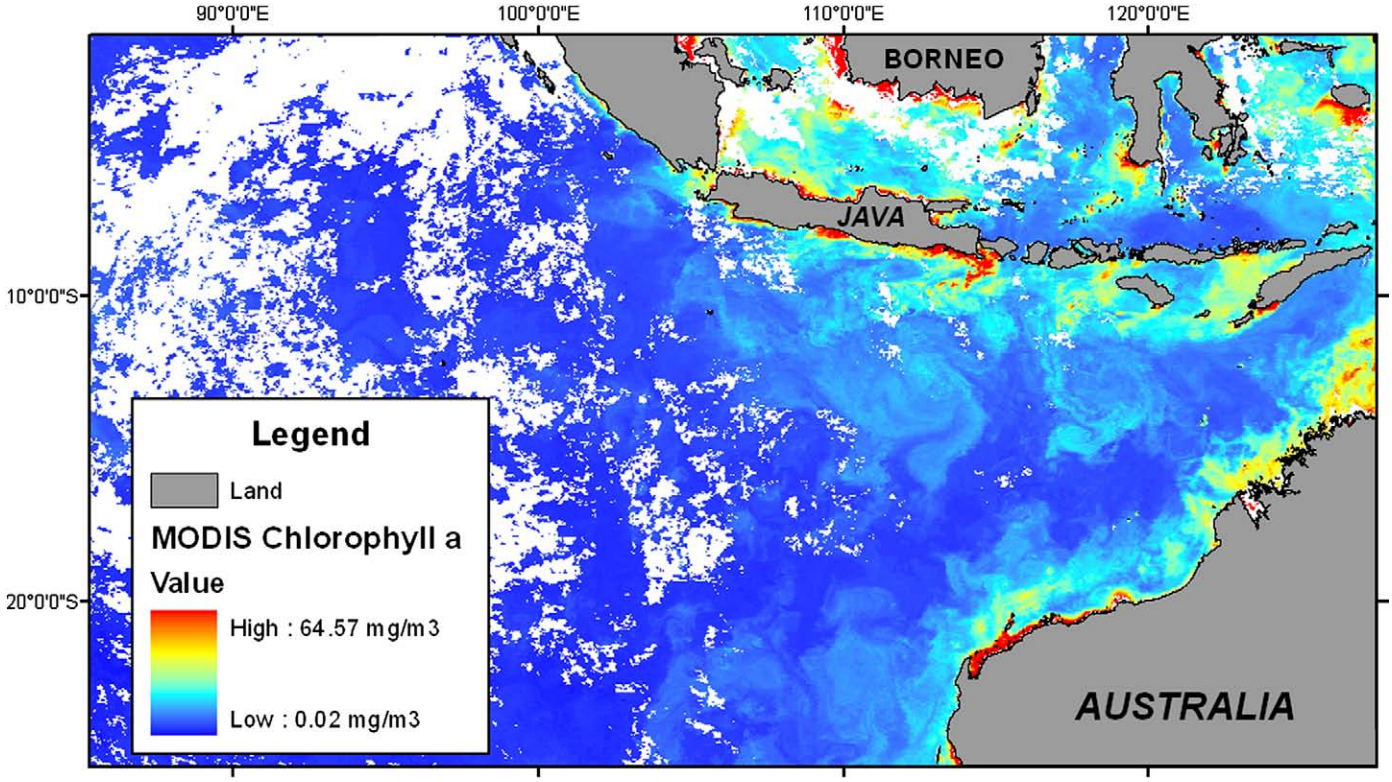

Fig. 3. Example of chlorophyll-*a* concentration map for the mid-winter period (June 2005).

the observed probability distributions of sharks using GridSampler (CSIRO Sustainable Ecosystems, Canberra, Australia).

2.4. Analysis

To test for a correlation between current speed and direction and the productivity surrogate on shark movement patterns, we constructed a set of five generalized linear mixed-effects models (GLMM) that incorporated these terms. We first assessed the amount of temporal autocorrelation between weekly values of the observed probability of occupying a grid cell.

We transformed the predicted probabilities for the observed and passive-movements accordingly using the complementary log–log transformation, and chlorophyll-*a* values with a $\log_{10}$ transformation

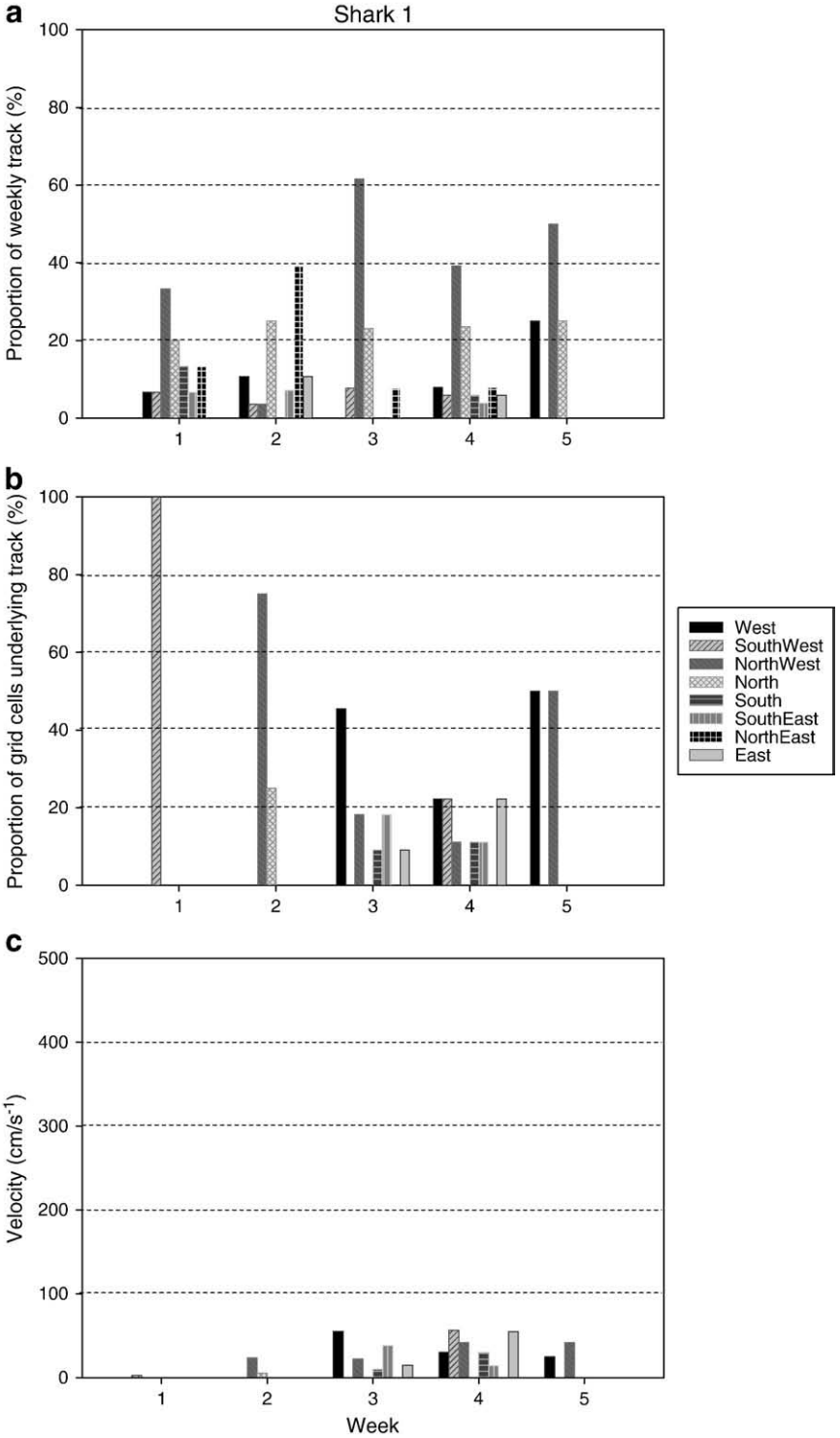

Fig. 4. a. Average heading direction (relative to True North) for Shark 1, b. Geostrophic current direction surrounding the tracks of Shark 1, c. Geostrophic current velocity (cm/s^{-1}) surrounding the tracks of Shark 1.

to normalise non-Gaussian distributions. Predicted probabilities for passive-movements were somewhat problematic given the large number of zero values. However, subsequent verification of the quantile–quantile plots indicated only minor departure from normality. Consequently, we constructed five *a priori* GLMM with the term *individual* coded as a random effect to account for repeated measurements (weekly values) per individual tracked. The response variable was the observed cell occupation probability, with model variants

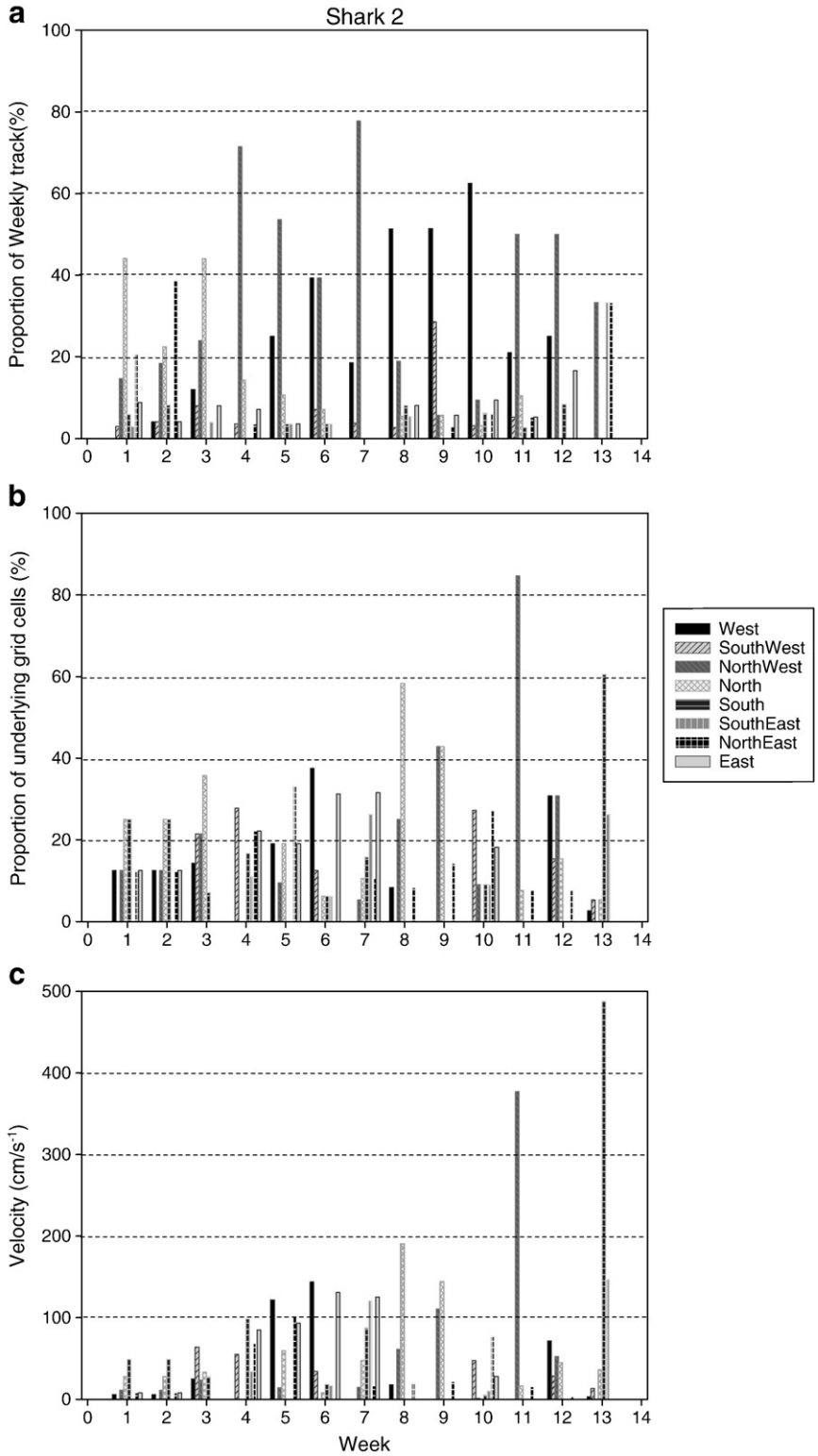

Fig. 5. a. Average heading direction (relative to True North) for Shark 2, b. Geostrophic current direction surrounding the tracks of Shark 2, c. Geostrophic current velocity (cm/s^{-1}) surrounding the tracks of Shark 2.

combining the chlorophyll-*a* concentration, passive-movement probability and their interaction (see Results).

Models were contrasted using an index of Kullback–Leibler (K–L) information loss that assigns relative strengths of evidence to each model (Burnham and Anderson, 2002). We used the Akaike's Information Criterion corrected for small sample sizes (AIC_c) to contrast models. AIC_c provides measures of model parsimony to identify a model from a set of candidate models that minimize K–L information loss (Burnham and Anderson, 2004), with the relative likelihoods of candidate models assessed using AIC_c weights. We also

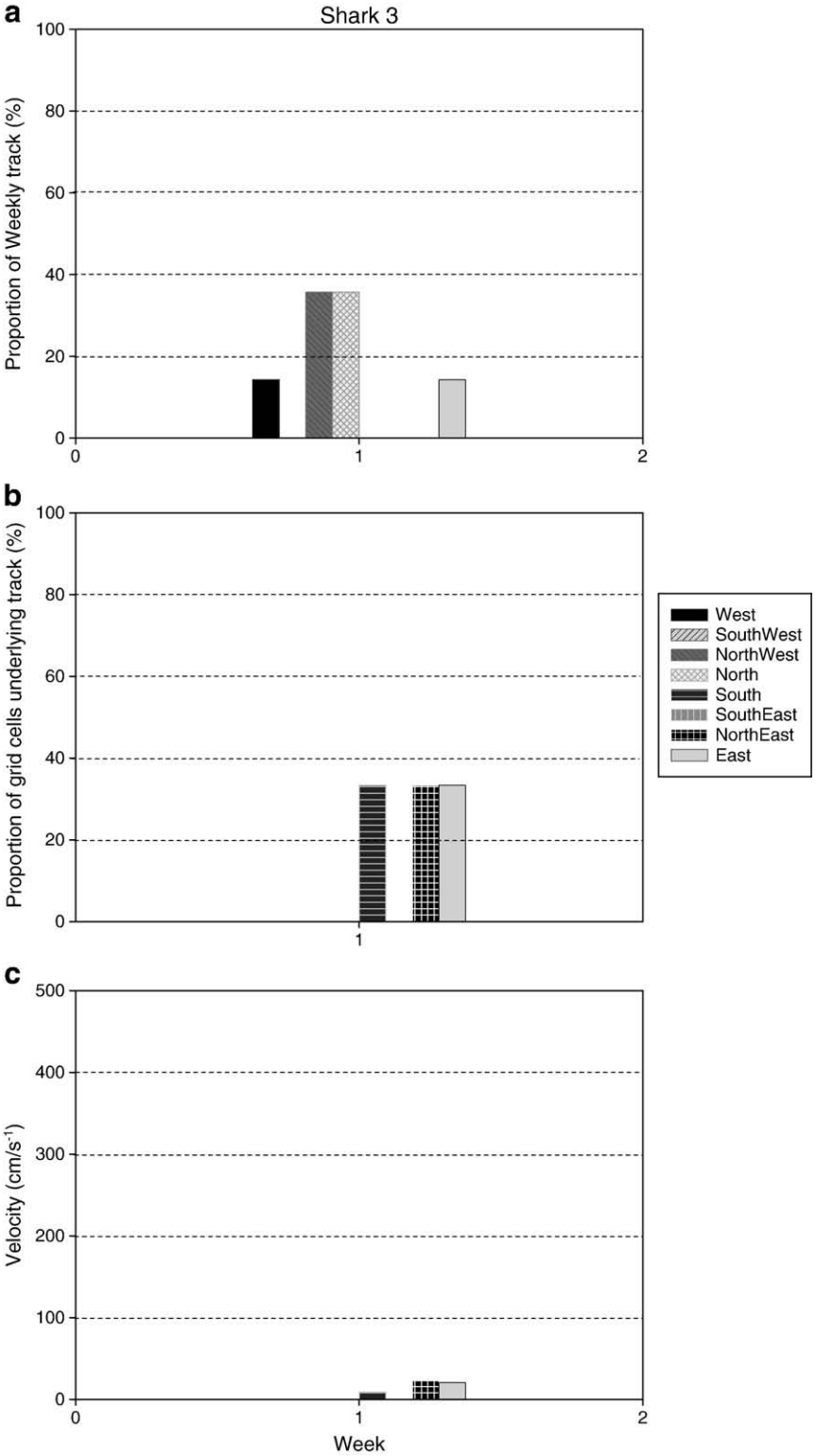

Fig. 6. a. Average heading direction (relative to True North) for Shark 3, b. Geostrophic current direction surrounding the tracks of Shark 3, c. Geostrophic current velocity (cm/s^{-1}) surrounding the tracks of Shark 3.

applied the dimension-consistent Bayesian Information Criterion (BIC) because the K–L prior used to justify AIC weighting can favour more complex models when sample sizes are large (Burnham and Anderson, 2004; Link and Barker, 2006). Thus, the weight ($wAIC_c$ and wBIC) of any particular model varies from 0 (no support) to 1 (complete support) relative to the entire model set. Model goodness-of-fit was assessed by calculating the per cent deviance explained (% DE) by a model relative to the null (Table 1).

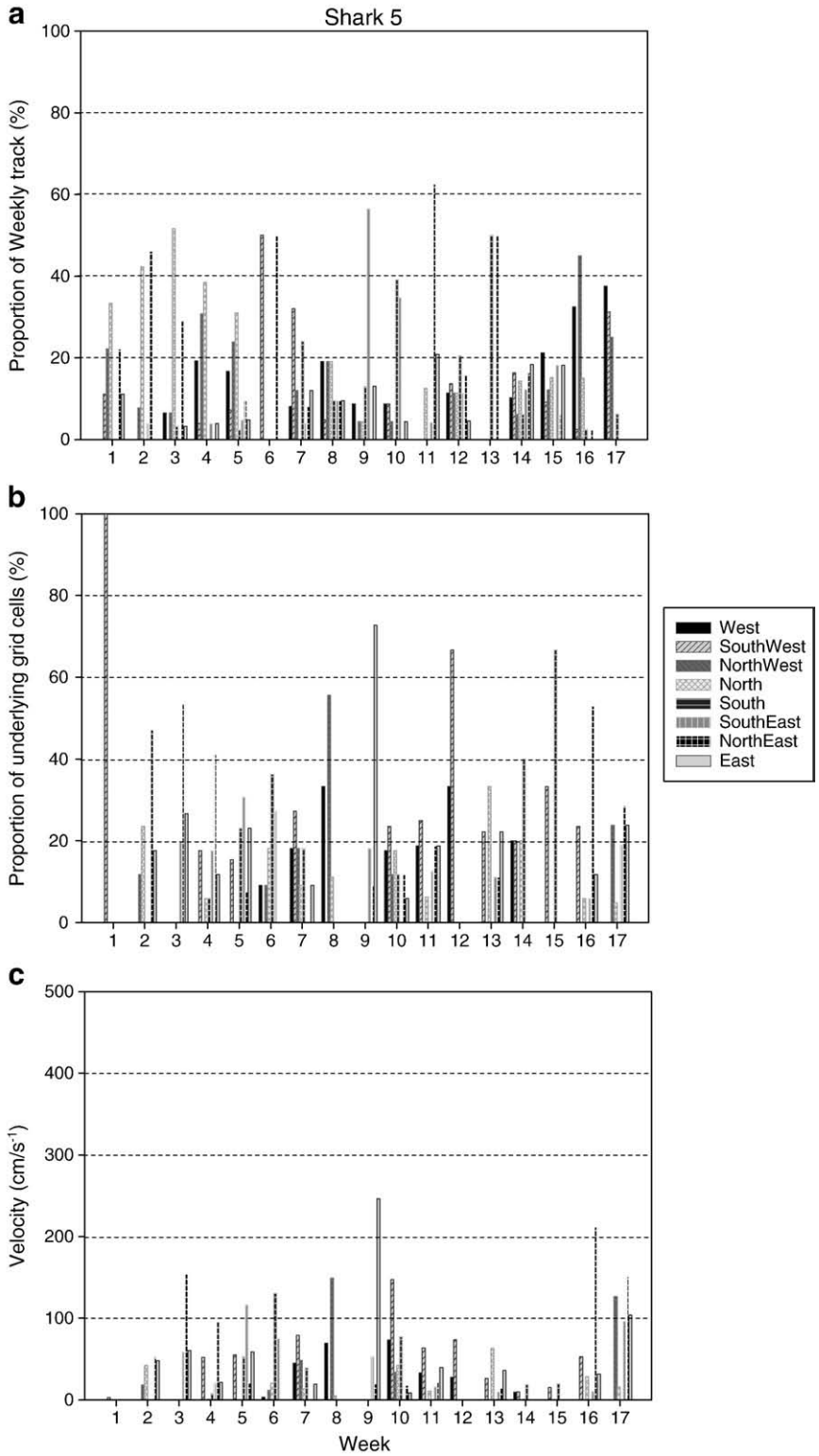

Fig. 7. a. Average heading direction (relative to True North) for Shark 5, b. Geostrophic current direction surrounding the tracks of Shark 5, c. Geostrophic current velocity (cm/s^{-1}) surrounding the tracks of Shark 5.

3. Results

Movements of the tagged whale sharks varied, but they generally traveled towards the equator (Fig. 1). When departing from Ningaloo Reef, two sharks (1 and 2) moved southward for approximately 270 km arriving near Dirk Hartog Island in Shark Bay before swimming in northwest arcs along the edge of the continental shelf. When in oceanic waters (distances greater than ~100 km from the coast) most sharks maintained a generally consistent directional heading over time. The movements of shark 5 were

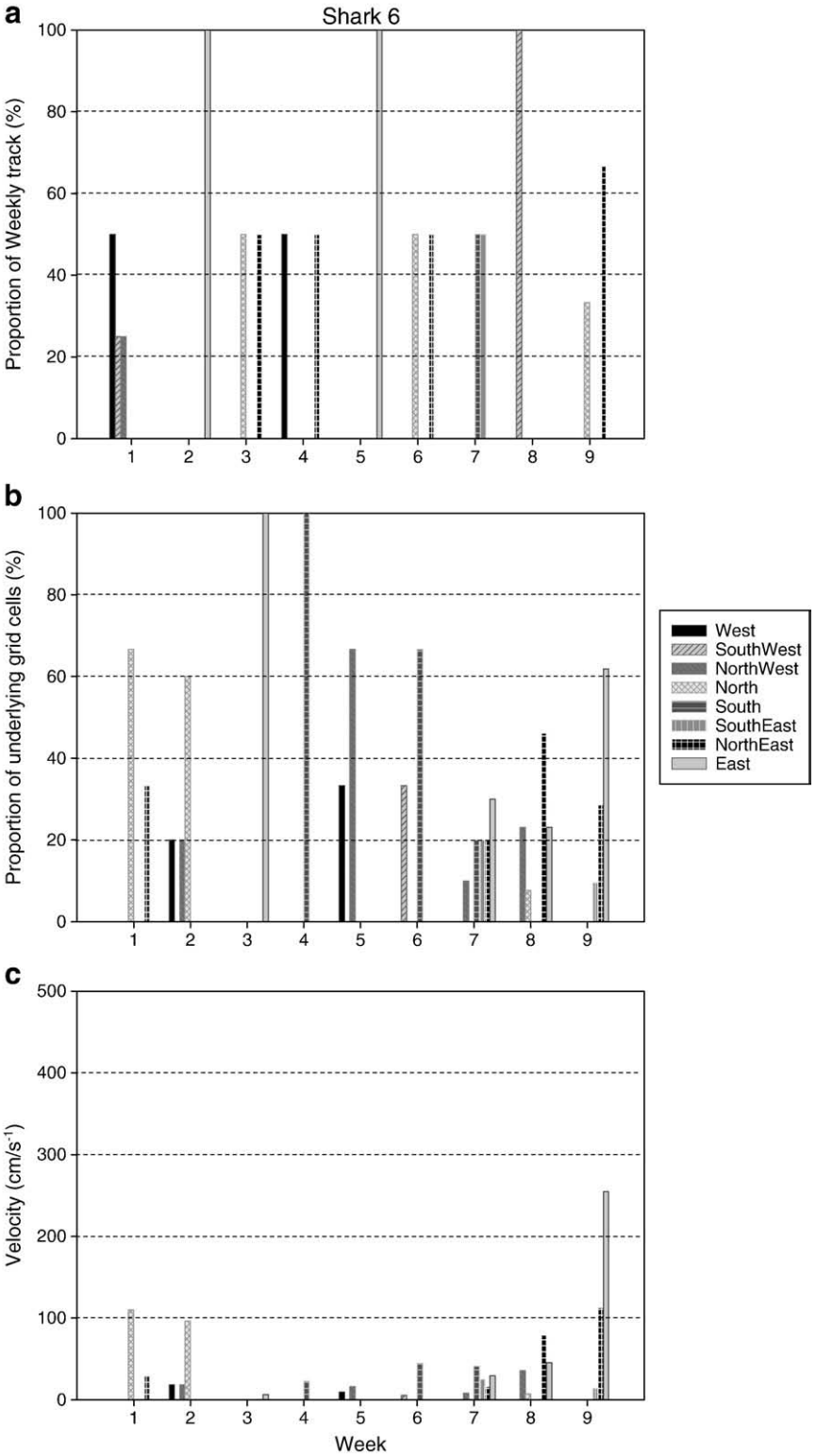

Fig. 8. a. Average heading direction (relative to True North) for Shark 6, b. Geostrophic current direction surrounding the tracks of Shark 6, c. Geostrophic current velocity (cm/s^{-1}) surrounding the tracks of Shark 6.

the most variable in terms of heading. It first moved north towards the southeast coast of Java in Indonesia, an area high in productivity, then circled around the shelf edge before returning to the mid ocean basin between Java and north western Australia. When almost 1500 km northwest of Ningaloo, shark 7 changed direction and headed east towards sea-mounts adjacent to Christmas Island (Fig. 1).

Velocities of geostrophic current throughout the northeast Indian Ocean ranged from 0 to 7.41 km h^{-1}, although whale sharks occurred in waters where currents did not exceed speeds greater than

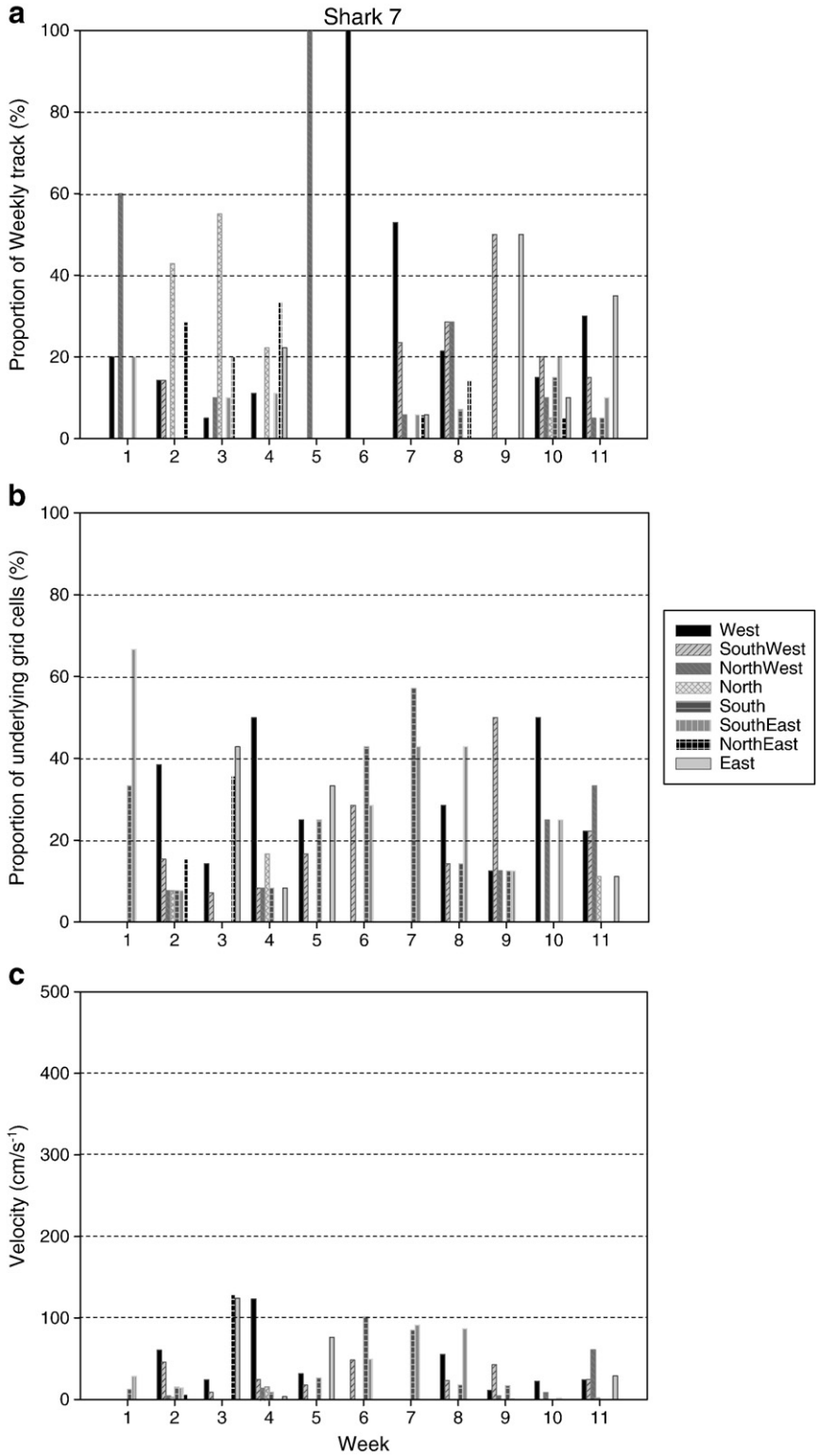

Fig. 9. a. Average heading direction (relative to True North) for Shark 7, b. Geostrophic current direction surrounding the tracks of Shark 7, c. Geostrophic current velocity (cm/s^{-1}) surrounding the tracks of Shark 7.

1.81 km h^{-1} (Table 2). The movement speeds of sharks averaged between 1.2 and 3.2 km h^{-1}, up to 3 times faster than the maximum velocities of geostrophic currents they encountered (Table 2).

Though regional directions of geostrophic currents varied substantially during the tracking period, cyclonic eddy systems (spiraling in clock-wise directions) and adjacent anti-cyclonic eddies (usually around 350 km to the west of cyclonic eddies) in the mid ocean basin between Java and Western Australia (see Fig. 2) were often prominent oceanographic features. These eddies usually corresponded with visible regions of biological productivity as

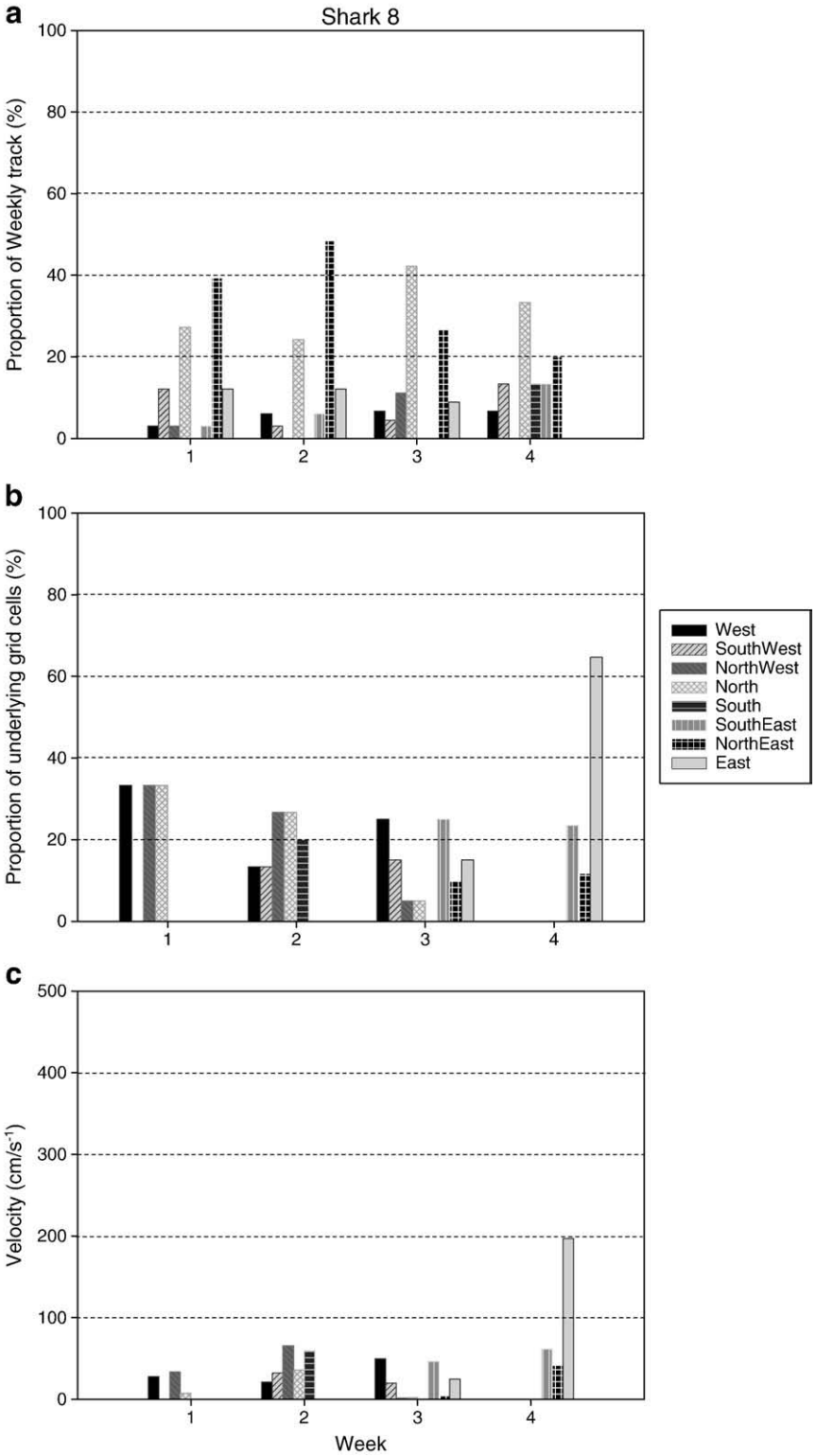

Fig. 10. a. Average heading direction (relative to True North) for Shark 8, b. Geostrophic current direction surrounding the tracks of Shark 8, c. Geostrophic current velocity (cm/s^{-1}) surrounding the tracks of Shark 8.

indicated by moderate near-surface chlorophyll-*a* (0.2–0.5 mg/m^3, see Fig. 3).

The movements of whale sharks corresponded poorly with the probability distribution maps from the passive diffusion model using geostrophic currents. Average weekly headings (relative to true North) of individual whale sharks varied widely and rarely correlated with the prevailing geostrophic current direction, even when current velocities were high <200 cm/s^{-1} (Figs. 4–10). Shark 1 spent a large proportion of weeks heading Northwest (Fig. 4a) while shark 2 spent the greatest proportion of each week moving in either a Northwest and/or Westerly direction, aside from initial few weeks where it moved mostly North (Fig. 5a). A strong Northwest flowing geostrophic current (velocity = 377 cm/s^{-1}) appeared to be utilized by shark 2 in week 11 of the study, (Fig. 5b), but otherwise there was little to indicate that other sharks were utilizing the prevailing geostrophic currents for movement. Shark 8 spent a large proportion of weeks heading North and/or Northeast (Fig. 10a).

Similarly, the movements of whale sharks corresponded poorly with the probability distribution maps from the passive diffusion model using geostrophic currents. Fig. 11a–f shows the cumulative tracks of individual whale sharks from satellite tags compared to probability distribution maps of tracks based on modelled passive diffusion by geostrophic currents. These modelled maps were parameterised with weekly starting points of whale sharks.

The generalized linear mixed-effects models indicated that the variables that we considered (passive-movement predicted cell occupancy probability and near-surface chlorophyll-*a*) accounted for only a small amount of the deviance in probabilities of observed cell occupancies (Table 1). Although there was reasonable support for a weak effect of chlorophyll-*a* (Table 1, Model 2 $wAIC_c = 0.371$, $wBIC = 0.686$), this only accounted for 0.8% of the deviance in the response. The addition of passive-movement probability was supported only by AIC_c ($wAIC_c = 0.432$) however, the extra deviance explained by this addition was minimal (~0.2%), and *w*BIC for this model was low (0.086). Examination of the partial residual plots for both terms (Fig. 12) revealed only a weak relationship with chlorophyll-*a*, but due to the highly skewed distribution (i.e., zero-dominated) of passive-movement probabilities, the correlation with observed cell occupancy probabilities was equivocal.

We applied the `acf` function in the *R* Package (R Development Core Team, 2004) to each of the observed cell probability time series for each shark. All `acf` lag probabilities fell within the 95% confidence interval for the uncorrelated series for all but shark 14, where there was a possible temporal autocorrelation at a lag of two weeks (data not shown). However, the lack of any strong evidence for important lags in these time series suggests that the assumption of independence was not violated.

4. Discussion

Despite evidence that some marine vertebrates use near-surface currents to aid their migration (Polovina et al., 2000, 2004; Luschi et al., 2003), we found that surface geostrophic currents explained only a small amount of the variation in the movements of whale

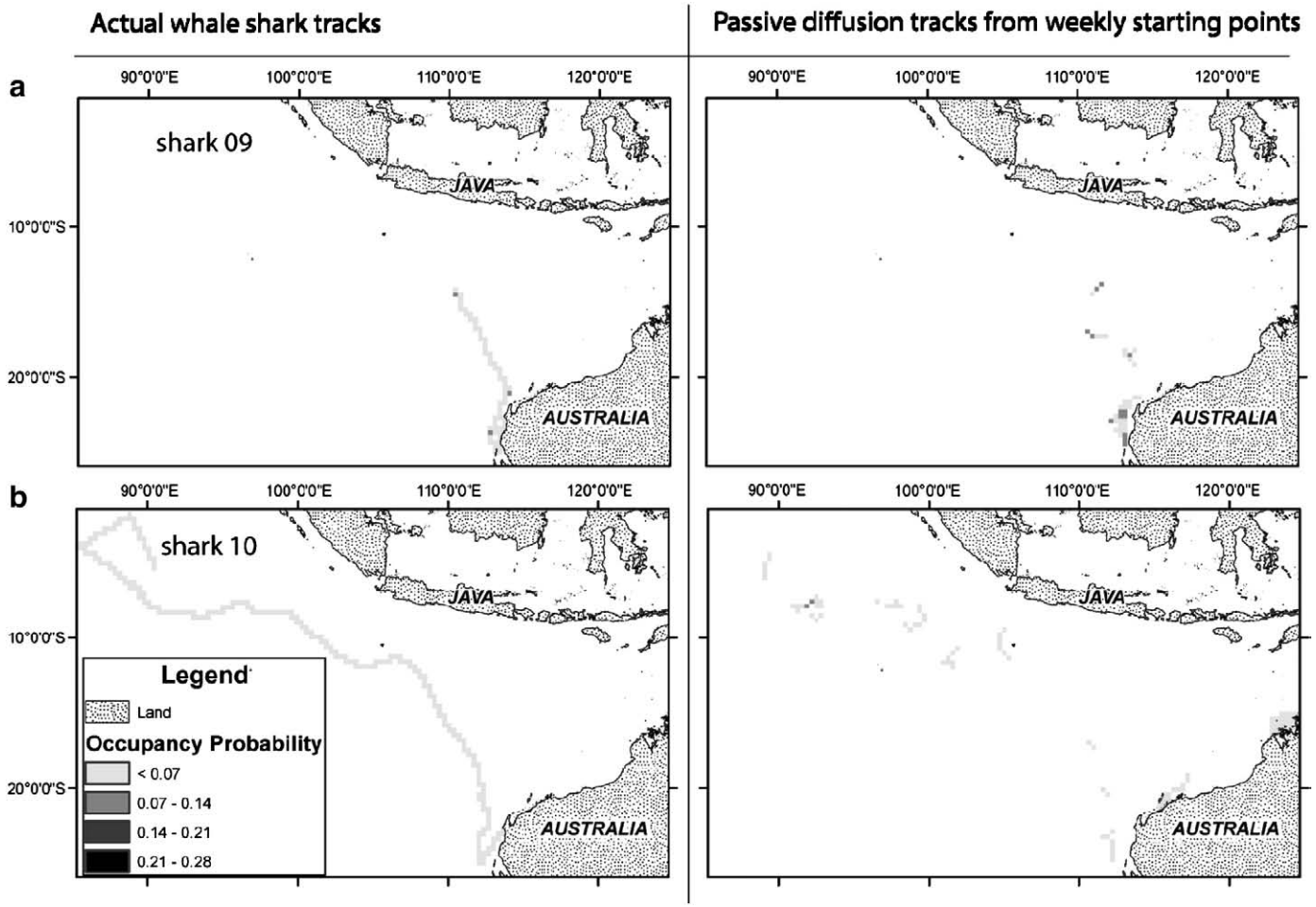

Fig. 11. a–f. Actual cumulative tracks of individual whale sharks (left) compared with probability distribution maps based on modelled passive diffusion by geostrophic currents (right). The modelled maps are parameterised with weekly starting points of whale sharks.

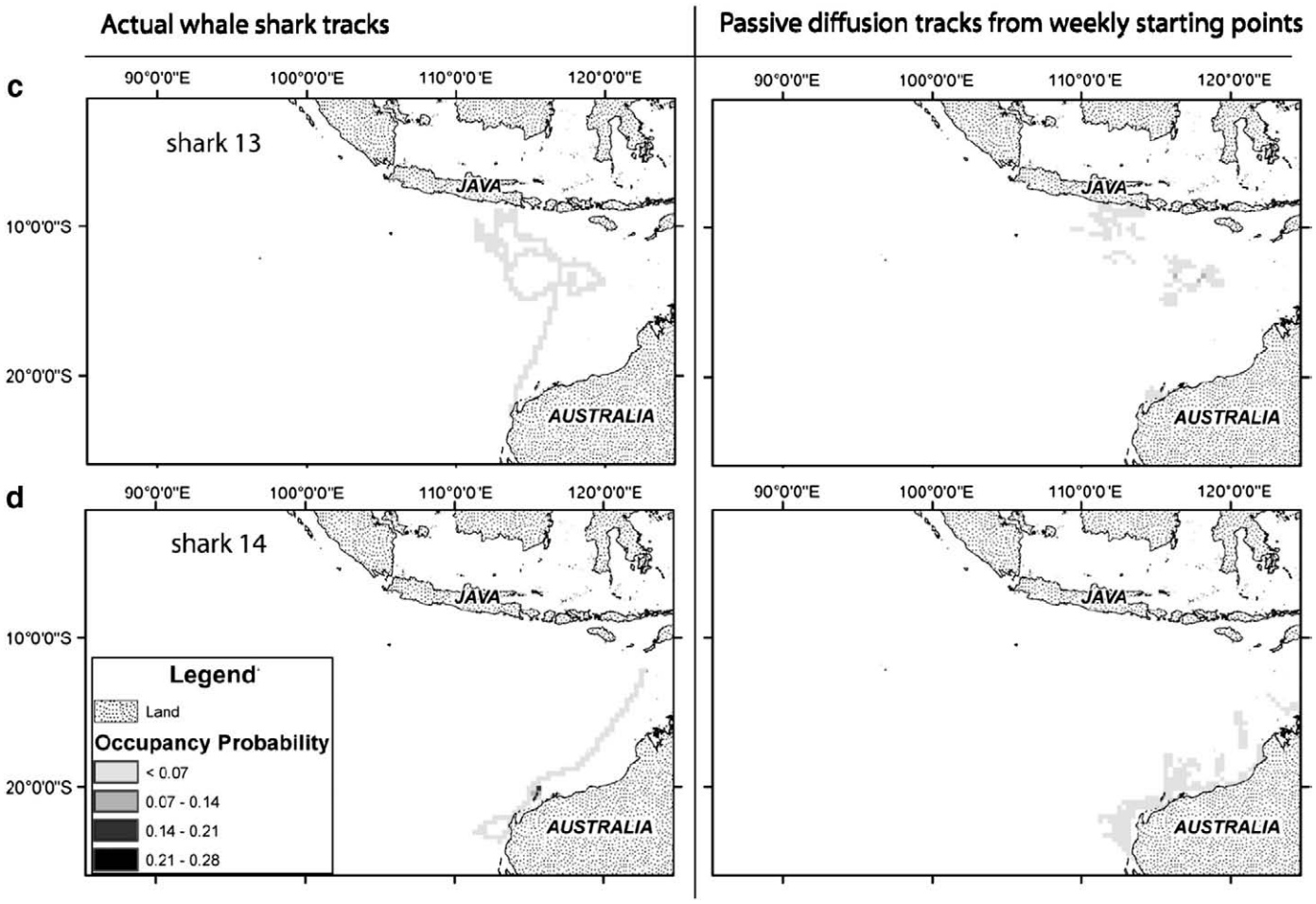

Fig. 11 (*continued*).

sharks that we tracked from Ningaloo Reef. The swimming speeds of those sharks were similar to other whale sharks tracked from Ningaloo (Gunn et al., 1999), the Eastern Pacific (Eckert and Stewart, 2001), South China Sea (Eckert et al., 2002a), Red Sea (Rowat et al., 2007), and the northwest Pacific (Hsu et al., 2007). Our tracked individuals swam generally much faster than average or maximum geostrophic current velocities they encountered. The combined current speed and direction data embedded within the stochastic passive diffusion model confirmed that whale sharks can effectively swim against prevailing surface currents and the sharks show little evidence of seeking out areas where surface currents might have otherwise favoured their movement.

Active swimming against currents will likely be more energetically costly to whale sharks compared to moving with currents. Whale sharks at Ningaloo Reef often feed actively (i.e. open-mouth lunging, slowly making tight circles around prey species) near-surface suggesting that foraging for subsequent migration is an important reason for whale shark seasonal aggregations at this locality.

The lack of a strong correlation between whale shark movement patterns and surface productivity as measured by chlorophyll-*a* concentrations suggests either (i) they exhibit little selective foraging behaviour or (ii) that chlorophyll-*a* is poor proxy for zooplankton biomass due to potential disparities between the distributions and life histories of particular types of phytoplankton and zooplankton assemblages (McKinnon and Duggan, 2001; Rossi et al., 2006). Limitations of satellite data associated with the depth of light penetration in sea-water may have biased this index of chlorophyll-*a* through omission or under-representation of phytoplankton biomass at increasing depth. Hydroacoustic sampling along Ningaloo Reef during summer has demonstrated that the deep chlorophyll maximum layer lies between depths of 60 and 100 m, whereas the SeaWiFS and MODIS data only account for chlorophyll-*a* in the layer between 0 and ~45 m from the surface (depending on atmospheric and bio-optical effects in the water column) (Yan et al., 2001; Wilson et al., 2002). This disassociation may indicate that whale sharks are foraging on subsurface food that is not directly evident from remotely sensed data, unlike the prey of basking sharks that are readily observed at the surface and are easily predicted from remote sensing (Sims and Merrett, 1997; Sims and Quayle, 1998).

After departing from Ningaloo, whale sharks consistently moved towards the equator and along the continental shelf of north Western Australia suggesting that their movements are non-random and perhaps related to continued active foraging independent of sea-surface currents. Although the routes taken varied among individuals, each shark tended to remain on an approximately consistent course. This suggests that whale sharks do not adopt random searching behaviours to maximize prey encounters, but may instead be responding to some larger-scale stimulus such as directed travel (Bradshaw et al., 2004; Hays et al., 2004).

Elasmobranchs are thought to rely on olfactory stimuli for middle-scale navigation and orientation, but they may also use these senses to navigate over long distances (Montgomery and Walker, 2001). Sound and magnetic fields might also be important for navigation cues to whale sharks (Klimley, 1993; Lohmann and Lohmann, 1996; Montgomery and Walker, 2001; Myrberg, 2001). Identifying and

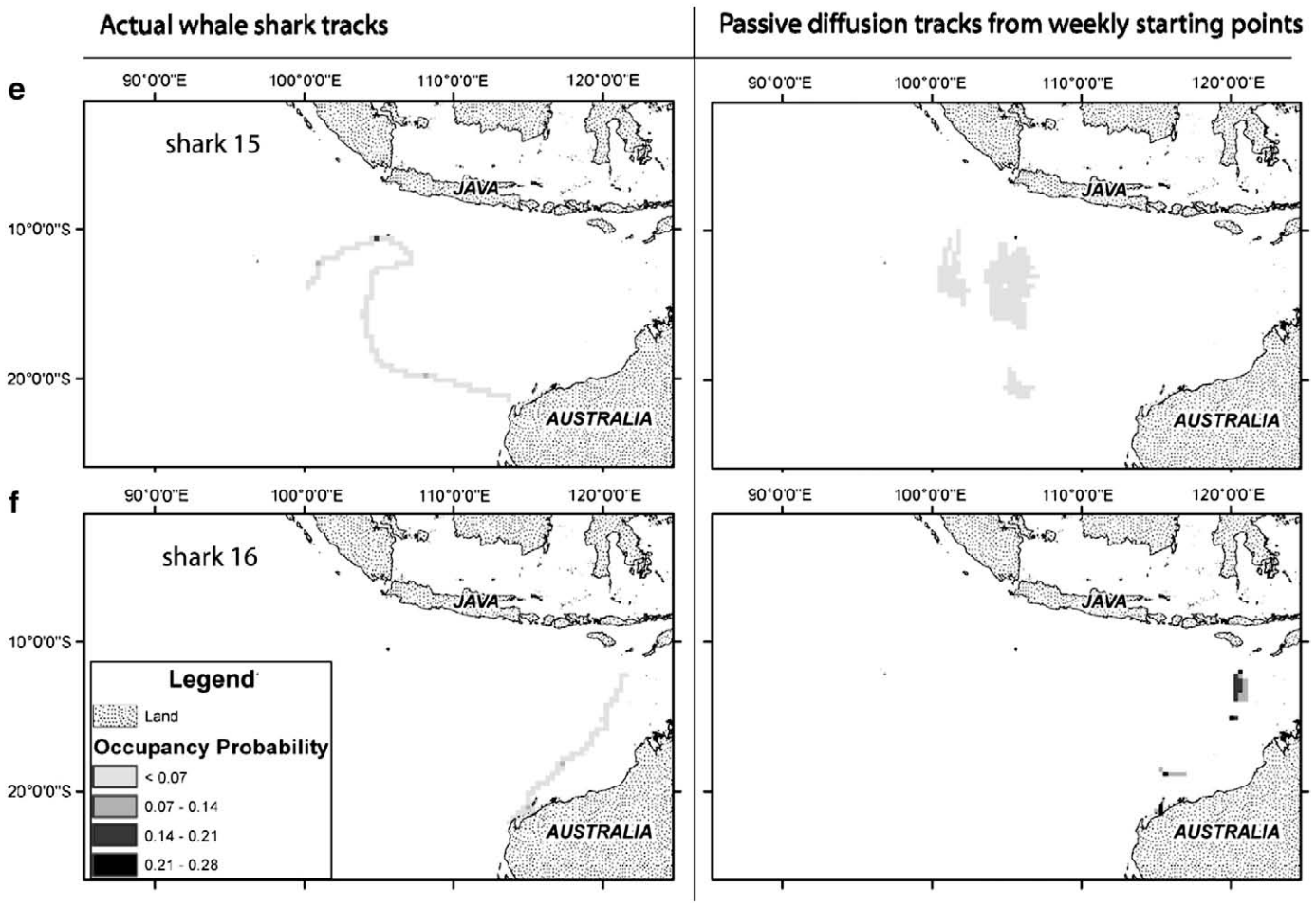

Fig. 11 (*continued*).

understanding the involvement of those cues will require longer term monitoring of movement patterns.

Future studies of whale shark movements and migration should look to engineering tags for prolonged retention, so that movement and behaviour can be understood within the context of specific life-history phases (e.g. Field et al., 2005). Further, better tracking technology should allow for the collection of more behavioural data that will help to distinguish feeding behaviours from other activities (Robinson et al., 2007). Moreover, that information will help develop a framework for evaluating habitat requirements of whale sharks to promote effective regional and global conservation.

Overall, our study found little support for geostrophic currents acting as passive dispersal mechanisms to whale sharks in the northwest Indian Ocean, with the caveat that we used broad-scale (0.1° grids at weekly intervals) data that may mask potential influences of these currents on whale shark distributions at smaller scales (i.e. kms at daily intervals). Alternatively, inherent limitations associated with tag (i.e. geolocation and triangulation algorithms) and/or geostrophic data (i.e., generalisation of values within 0.1° grid cells) may have contributed to the lack of support for geostrophic transport in whale shark movement. Other studies have indicated lack of correspondence between historical ship drift and geostrophic currents, particularly in equatorial waters and suggest that additional information on wind stress and vertical viscosity can help improve, but not necessarily approximate a model to explain surface current drift (Arnault, 1987). While there are no remotely sensed data available for measuring vertical viscosity of the northwest Indian Ocean, new models approximating wind stress (from altimetry) could be included in future investigations.

Regardless of the accuracy of surface current data, whale sharks in the northeast Indian Ocean are likely to be actively foraging rather than simply transiting through areas of ocean. This premise is supported by results of PAT tag studies showing diurnal and nocturnal vertical migration, characteristic of feeding behaviour (Wilson et al., 2006). Given that this is the case, we need to more closely identify and analyse the relationships between dive locations and biophysical parameters within the water column, across whale shark migration routes at various spatial and temporal scales.

Acknowledgements

We thank C. McLean (AIMS), M. Horsham (CSIRO Marine & Atmospheric Research), G. Taylor and T. Maxwell for assistance in the field and M. Horsham for his design and modification of the satellite tag applicator. We also thank the R. Mau and the Western Australian Department of Environment and Conservation (formerly CALM) for their logistic assistance and T. Maxwell for support from his vessel *Osso Blue*. This research was supported by funding from the Australian Institute of Marine Science, CSIRO Marine and Atmospheric Research, BHP Billiton Ltd., Woodside Energy Ltd., Chevron, U.S. NOAA Fisheries, DEC and Hubbs-SeaWorld Research Institute. **[SS]**

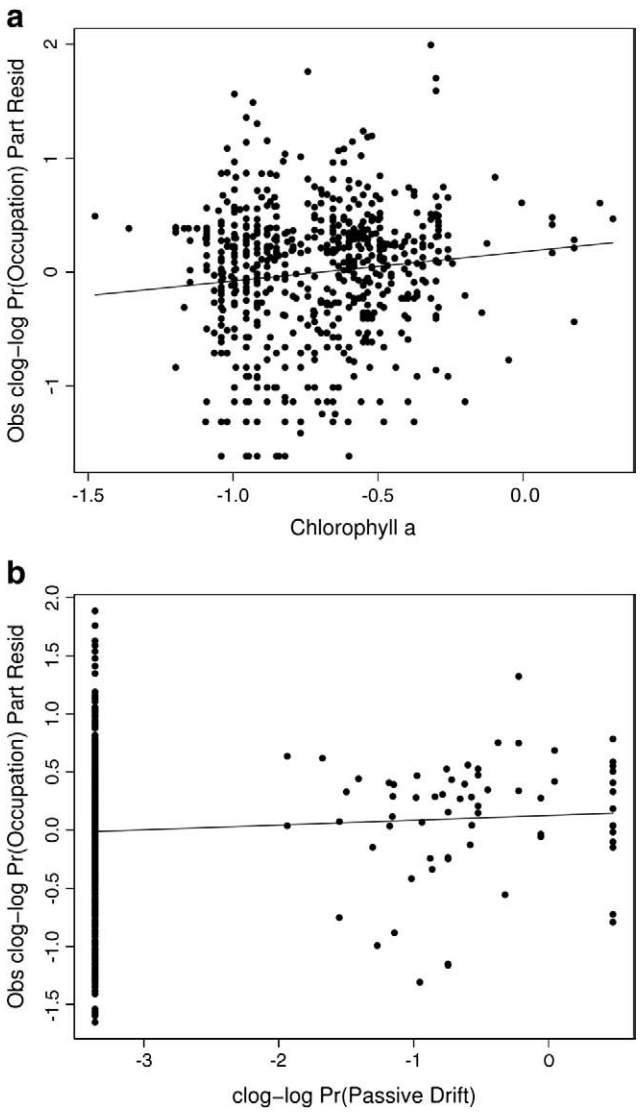

Fig. 12. Partial residual plots of the relationship between the complementary log–log (clog–log) of the observed cell occupancy probability and the (a) log of chlorophyll-*a* concentration and (b) the clog–log of the passive-movement predicted cell occupancy probability.

References

Arnault, S., 1987. Tropical Atlantic geostrophic currents and ship drifts. J. Geophys. Res. C 92, 5076–5088.

Ballance, L.T., Pitman, R.L., Fiedler, P.C., 2006. Oceanographic influences on seabirds and cetaceans of the eastern tropical Pacific: a review. Prog. Oceanogr. 69, 360–390.

Bradshaw, J.A., Higgins, J., Michael, K., Wotherspoon, S.J., Hindell, M.A., 2004. At-sea distribution of female southern elephant seals relative to variation in ocean surface properties. ICES J. Mar. Sci. 61, 1014–1027.

Burnham, K.P., Anderson, D.R., 2002. Model Selection and Multimodal Inference: A Practical Information-Theoretic Approach. Springer-Verlag, New York, USA. 488 pp.

Burnham, K.P., Anderson, D.R., 2004. Understanding AIC and BIC in model selection. Sociol. Methods Res. 33, 261–304.

Eckert, S.A., Stewart, B.S., 2001. Telemetry and satellite tracking of whale sharks, *Rhincodon typus*, in the Sea of Cortez, Mexico, and the North Pacific Ocean. Environ. Biol. Fishes 60, 299–308.

Eckert, S.A., Dolar, L.L., Kooyman, G.L., Perrin, W., Rahman, R.A., 2002a. Movements of whale sharks (*Rhincodon typus*) in South-east Asian waters as determined by satellite telemetry. J. Zool. A 257, 111–115.

Field, I.C., Bradshaw, C.J.A., Burton, H.R., Sumner, M.D., Hindell, M.A., 2005. Resource partitioning through oceanic segregation of foraging juvenile southern elephant seals. Oecologia 142, 127–135.

Gaspar, P., Georges, J.-Y., Fossette, S., Lenoble, A., Ferraroli, S., Maho, Y.L., 2006. Marine animal behaviour: neglecting ocean currents can lead us up the wrong track. Proc. R. Soc. Biol. Sci. Ser. B 273, 2697–2702.

Gunn, J.S., Stevens, J.D., Davis, T.L.O., Norman, B.M., 1999. Observations on the short-term movements and behaviour of whale sharks (*Rhincodon typus*) at Ningaloo Reef, Western Australia. Mar. Biol. 135, 553–559.

Hays, G.C., Houghton, J.D.R., Myers, A.E., 2004. Endangered species: Pan-Atlantic leatherback turtle movements. Nature 429, 522.

Heyman, W.D., Graham, R.T., Kjerfve, B., Johannes, R.E., 2001. Whale sharks *Rhincodon typus* aggregate to feed on fish spawn in Belize. Mar. Ecol. Prog. Ser. 215, 275–282.

Hsu, H.-H., Joung, S.-J., Liao, Y.-Y., Liu, K.-M., 2007. Satellite tracking of juvenile whale sharks, *Rhincodon typus*, in the Northwestern Pacific. Fish. Res. 84, 25–31.

Klimley, A.P., 1993. Highly directional swimming by scalloped hammerhead sharks, *Sphyrna lewini*, and subsurface irradiance, temperature, bathymetry, and geomagnetic field. Mar. Biol. 117, 1–22.

Lambardi, P., Lutjeharms, J.R.E., Mencacci, R., Hays, G.C., Luschi, P., 2008. Influence of ocean currents on long-distance movement of leatherback sea turtles in the Southwest Indian Ocean. Mar. Ecol. Prog. Ser. 353, 289–301.

Link, W.A., Barker, R.J., 2006. Model weights and the foundations of multimodel inference. Ecology 87, 2626–2635.

Lohmann, K.J., Lohmann, C.M.F., 1996. Detection of magnetic field intensity by sea turtles. Nature 380, 59.

Luschi, P.L., Hays, G.C., Papi, F., 2003. A review of long-distance movements by marine turtles, and the possible role of ocean currents. Oikos 103, 293–302.

McKinnon, A.D., Duggan, S., 2001. Summer egg production rates of paracalanid copepods in subtropical waters adjacent to Australia's North West Cape. Hydrobiologia 453 (454), 121–132.

Meekan, M.G., Bradshaw, C.J.A., Press, M., McLean, C., Richards, A., Quasnichka, S., Taylor, J.G., 2006. Population size and structure of whale sharks (*Rhincodon typus*) at Ningaloo Reef, Western Australia. Mar. Ecol. Prog. Ser. 319, 275–285.

Montgomery, J.C., Walker, M.M., 2001. Orientation and navigation in elasmobranchs: which way forward? Environ. Biol. Fishes 60, 109–116.

Myrberg, A.A.J., 2001. The acoustical biology of elasmobranchs. Environ. Biol. Fishes 60, 31–45.

O'Neill, R.V., Hunsaker, C.T., Timmins, S.P., Jackson, B.L., Jones, K.B., Riitters, K.H., Wickham, J.D., 1996. Scale problems in reporting landscape pattern at the regional scale. Landsc. Ecol. 11, 169–180.

Polovina, J.J., Kleiber, P., Kobayashi, D.R., 1999. Application of TOPEX-POSEIDON satellite altimetry to simulate transport dynamics of larvae of spiny lobster, *Panulirus marginatus*, in the Northwestern Hawaiian Islands, 1993–1996. Fish Bull. 97, 132–143.

Polovina, J.J., Kobayashi, D.R., Ellis, D.M., Seki, M.P., Balaz, G.H., 2000. Turtles on the edge: movement of loggerhead turtles (*Caretta caretta*) along oceanic fronts in the central North Pacific, 1997–1998. Fish. Oceanogr. 9, 71–82.

Polovina, J.J., Balazs, G.H., Howell, E.A., Parker, D.M., Seki, M.P., Dutton, P.H., 2004. Forage and migration habitat of loggerhead (*Caretta caretta*) and olive ridley (*Lepidochelys olivacea*) sea turtles in the central North Pacific Ocean. Fish. Oceanogr. 13, 36–51.

R Development Core Team, 2004. R: A Language and Environment for Statistical Computing. R Foundation for Statistical Computing, Vienna, Austria.

Rio, M.H., Hernandez, F., 2004. A mean dynamic topography computed over the world ocean from altimetry, in situ measurements, and a geoid model. J. Geophys. Res. 109, 1–19.

Robinson, P.W., Tremblay, Y., Crocker, D.E., Kappes, M.A., Kuhn, C.E., Shaffer, S.A., Simmons, S.E., Costa, D.P., 2007. A comparison of indirect measures of feeding behaviour based on argos tracking data. Deep Sea Res. Part II, 54, 356–368. doi:10.1016/j.dsr2.2006.11.020.

Rossi, S., Sabates, A., Latasa, M., Reyes, E., 2006. Lipid biomarkers and trophic linkages between phytoplankton, zooplankton and anchovy (*Engraulis encrasicolus*) larvae in the NW Mediterranean. J. Plankton Res. 28, 551–562.

Rowat, D., Gore, M., 2007. Regional scale horizontal and local scale vertical movements of whale sharks in the Indian Ocean off Seychelles. Fish. Res. 84, 32–40.

Rowat, D., Meekan, M.G., Engelhardt, U., Pardigon, B., Vely, M., 2007. Aggregations of juvenile whale sharks (*Rhincodon typus*) in the Gulf of Tadjoura, Djibouti. Environ. Biol. Fish. 80, 465–472. doi:10.1007/s10641-006-9148-7.

Shillinger, G.L., Palacios, D.M., Bailey, H., Bograd, S.J., Swithenbank, A.M., Gaspar, P., Wallace, B.P., Spotila, J.R., Paladino, F.V., Piedra, R., Eckert, S.A., Block, B.A., 2008. Persistent leatherback turtle migrations present opportunities for conservation. PLoS Biol. 6, 1408–1416.

Sims, D.W., 2003. Tractable models for testing theories about natural strategies: foraging behaviour and habitat selection of free-ranging sharks. J. Fish Biol. 63, 53–73.

Sims, D.W., Merrett, D.A., 1997. Determination of zooplankton characteristics in the presence of surface feeding basking sharks cetorhinus maximus. Mar. Ecol. Prog. Ser. 158, 297–302.

Sims, D.W., Quayle, V.A., 1998. Selective foraging behaviour of basking sharks on zooplankton in a small-scale front. Nature 393, 460–464.

Sims, D.W., Southall, E.J., Merrett, D.A., Sanders, J., 2003. Effects of zooplankton density and diel period on surface-swimming duration of basking sharks. J. Mar. Biol. Assoc. UK 83, 643–646.

Stewart, B.S., Leatherwood, S., Yochem, P.K., Heide-Jorgensen, M.P., 1989. Harbor seal tracking and telemetry by satellite. Mar. Mamm. Sci. 5, 361–375.

Tremblay, Y., Shaffer, S.A., Fowler, S.L., Kuhn, C.E., McDonald, B.I., Weise, M.J., Bost, C.-A., Weimerskirch, H., Crocker, D.E., Goebel, M.E., Costa, D.P., 2006. Interpolation of animal tracking data in a fluid environment. J. Exp. Biol. 209, 128–140.

Wilson, S.G., Taylor, J.G., Pearce, A.F., 2001. The seasonal aggregation of whale sharks at Ningaloo Reef, Western Australia: currents, migrations and the El Nino/ Southern Oscillation. Environ. Biol. Fishes 61, 1–11.

Wilson, S.G., Pauly, T., Meekan, M.G., 2002. Distribution of zooplankton inferred from hydroacoustic backscatter data in coastal waters off Ningaloo Reef, Western Australia. Mar. Freshw. Res. 53, 1005–1015.

Wilson, S.G., Polovina, J.J., Stewart, B.S., Meekan, M.G., 2006. Movements of whale sharks (*Rhincodon typus*) tagged at Ningaloo Reef, Western Australia. Mar. Biol. 148, 1157–1166.

Yan, B., Stamnes, K., Toratani, M., Li, W., Stamnes, J.J., 2001. Evaluation of a reflectance model used in the SeaWiFS ocean color algorithm: implications for chlorophyll concentration retrievals. Appl. Opt. 41, 6243–6259.